

# Automatika

Journal for Control, Measurement, Electronics, Computing and Communications



ISSN: (Print) (Online) Journal homepage: [www.tandfonline.com/journals/taut20](http://www.tandfonline.com/journals/taut20)

## Online controller optimization for a voltage-doubler boost rectifier with high power factor

Jhon Bayona, Nancy Gélvez & Helbert Espitia

To cite this article: Jhon Bayona, Nancy Gélvez & Helbert Espitia (2024) Online controller optimization for a voltage-doubler boost rectifier with high power factor, *Automatika*, 65:4, 1421-1431, DOI: [10.1080/00051144.2024.2393042](https://doi.org/10.1080/00051144.2024.2393042)

To link to this article: <https://doi.org/10.1080/00051144.2024.2393042>



© 2024 The Author(s). Published by Informa UK Limited, trading as Taylor & Francis Group.



[View supplementary material](#)



Published online: 29 Aug 2024.



[Submit your article to this journal](#)



Article views: 153



[View related articles](#)



[View Crossmark data](#)



# Online controller optimization for a voltage-doubler boost rectifier with high power factor

Jhon Bayona <sup>a</sup>, Nancy Gélvez <sup>b</sup> and Helbert Espitia <sup>b</sup>

<sup>a</sup>Facultad de Ingeniería, Universidad ECCI, Bogotá, Colombia; <sup>b</sup>Facultad de Ingeniería, Universidad Distrital Francisco José de Caldas, Bogotá, Colombia

## ABSTRACT

The design of converters is essential for the proper use of electrical energy. Half-bridge topology represents a suitable conversion scheme to implement a boost rectifier converter. Consequently, this article proposes the parameter optimization of a proportional-integral-derivative (with filter) controller for a half-bridge boost rectifier with a high power factor. Regarding the high simulation time for the converter, stochastic hill-climbing and simulated annealing algorithms are employed for the optimization process. The results display that the optimized controller allows suitable values for the power factor and output waveform. The controller parameters obtained through optimization algorithms result in a high power factor of 0.9934 when the half-bridge boost rectifier is operating at full load.

## ARTICLE HISTORY

Received 18 July 2023  
Accepted 5 August 2024

## KEYWORDS

Control; half-bridge boost converter; optimization; simulated annealing; stochastic hill climbing



## 1. Introduction

The proper use of energy is essential for power generation. Power conversion and consumption process must be as efficient as possible, which demands an adequate power converters design. Regarding control converter optimization, reference [1] shows the optimization of a PD (Proportional Derivative) fuzzy-type Takagi-Sugeno controller used to regulate the voltage of a single-phase DC-AC inverter. The fuzzy system is designed aiming to have a less number of parameters to be optimized. Meanwhile, paper [2] presents the optimization of a Power Factor Correction (PFC) Cuk converter for the minimization of Total Harmonic Distortion (THD) and voltage ripple. The authors designed a PFC Cuk converter for working in Discontinuous Conduction Mode (DCM) to obtain nearly unity power factor. Optimization is rooted in the energy compensation between the output inductor and the input capacitor to allow THD current minimization. According to [3], Selective Harmonic Elimination (SHE) is a suitable approach to suppress low-order harmonics. Authors of [3], to eliminate selective harmonics in cascaded multilevel inverters (5-level, 7-level, and 9-level), propose a modified version of the moth-flame algorithm to determine the optimum switching angles. As the main achievement, the low-order harmonics are suppressed.

Meanwhile, the authors in [4] present the online method for tuning five different fractional order controllers based on a reference tracking method. First Order With Dead Time (FOWDT) system is considered to inspect the controller viability. Besides, a battery

charger based on a Photovoltaic (PV) system is proposed in [5], consisting of a buck converter as a Photovoltaic module interface. At this point, optimization is essential since the output power of Photovoltaic devices quickly varies according to solar radiation; therefore, the authors propose a Perturb and Observe (P&O) algorithm to control the buck converter switch. Another work to consider is shown in [6] that presents a review of three dominant groups of multilevel inverters as: neutral point clamped, cascaded h-bridge, and flying capacitor. The authors show that harmonic elimination is conventionally addressed by controlling the inverter's switching angles, where Selective Harmonic Elimination Pulse Width Modulation (SHEPWM) approach is extensively employed. In this review is also identified the use of Particle Swarm Optimization (PSO) for tuning. Regarding converter applications, the temperature control considering the time of induction cooking is performed in [7] employing a Super Twisting Sliding Mode Control (ST-SMC) and Dynamic Particle Swarm Optimization (D-PSO) to optimize the gain values of the ST-SMC.

In order to meet IEC-61000-3-2 and IEEE Std 519 standards, the power factor corrected voltage-doubler boost rectifier is the most suitable alternative since it can provide double Direct Current (DC) output voltage and uses fewer switches compared to other rectifiers, which leads to higher efficiency. Some work on this rectifier with power factor correction has been done either to enhance the power factor or to solve the unbalance problem in the two output DC rails.

**CONTACT** Helbert Espitia  [heespitiac@udistrital.edu.co](mailto:heespitiac@udistrital.edu.co)  Facultad de Ingeniería, Universidad Distrital Francisco José de Caldas, Bogotá 110231, Colombia

A bidirectional buck-boost converter was proposed to correct this imbalance without lowering the power factor [8]. In addition, an isolated battery charger for electric vehicles, which uses two diodes in series and a minimum number of magnetic components, was presented to reduce the oscillation in discontinuous mode [9]. Finally, in [10] was designed a single-stage LED driver to obtain a high power factor, integrating a non-resonant half-bridge converter and a non-bridge boost rectifier.

Regarding comparison with other related works, the first paper to consider is [11], where the authors studied a high-frequency resonant AC-DC converter that employs an isolated dual-tank LCL to obtain a high power factor. The second reference is [12] as it presents the control of a single-phase and three-phase rectifier with power factor correction. A third work to consider is [13], where for a half-bridge rectifier (single-phase), near unity power factor and balancing voltages on each half of the DC bus are achieved through a nonlinear analog controller. Finally, reference [14] is considered since it employs a Multiple Particle Swarm Optimization (MPSO) algorithm to tune a Proportional Integral Derivative (PID) controller to correct the power factor in a boost topology AC-DC converter.

### 1.1. Proposal approach

This document aims at displaying the proposal for controller optimization for a voltage-doubler boost rectifier with a high power factor. In this order is employed heuristic based on an individual in such a way that it can be used for online optimization on a continuous basis.

Regarding optimization approaches [15, 16], heuristic algorithms allow a better exploration of the search space, however, population-based algorithms such as particle swarm and genetics algorithms result to be impractical since the calculation of the objective function for each individual is required. In this case, there exists a limitation in the evaluation of the objective function due to the dynamics (complexity) of the plant. In this order, considering the high simulation time of the model, a stochastic hill climbing and simulated annealing are employed as optimization algorithms since they are heuristic algorithms based on an individual and allow optimization without restarting the plant.

The objective of this work is to determine if the stochastic hill climbing and simulated annealing algorithms can be used with an online approach for the optimization of a PIDF controller in a power converter. This is done considering that this process can be used in an adaptive approach to adjust the controller parameters when a variation occurs in the converter.

The document is organized as follows: Section 2 qualitatively describes the circuit functioning. Following Section 3 presents some aspects of stochastic hill

climbing optimization. Meanwhile, Section 4 describes the simulated annealing algorithm. Later, Section 5 presents the optimization process. Then, the results of the converter optimization are presented in Section 6. Finally, the discussion and conclusions are given in Sections 7 and 8.

## 2. Circuit description

Figure 1 displays the voltage-doubler boost rectifier with power factor correction composed of two MOSFET transistors  $S_1$  and  $S_2$ , with their respective intrinsic diodes  $D_1$  and  $D_2$ , two capacitors  $C_1$  and  $C_2$ , an inductance  $L$  and a resistive load  $R$ .

The control scheme of the voltage-doubler boost rectifier in Figure 1 consists of three loops, namely current, sum voltage, and difference voltage. The current loop compensator is a PID with a filter (PIDF) with its own transfer function, and its purpose is that the input current of the rectifier  $i$  follow (tracking) line voltage  $v_g$  to obtain a power factor close to unity. The sum voltage loop compensator is a PI, and its objective is to keep  $v_s$  at a constant value defined by the reference value  $V_R$ . The difference voltage loop compensator is a block with constant gain  $k$ , and its purpose is to balance the capacitor voltages. According to [17], when the model is linearized, the respective transfer function displays a zero at the origin, which is why it is not possible to reach a zero steady-state error. Likewise, the input current cannot follow the current of reference; therefore, the  $P(s)$  block is a pre-compensator to decrease this

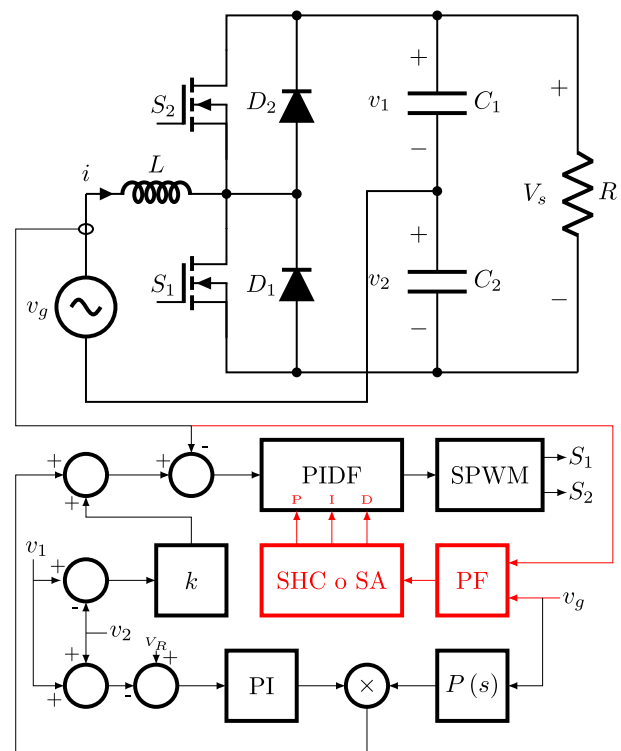


Figure 1. Voltage-doubler boost rectifier converter.

**Table 1.** Voltage-doubler boost rectifier parameter values.

Circuit parameter	Symbol	Value
Output capacitors	$C = C_1 = C_2$	100 $\mu$ F
Inductance	$L$	5 mH
Load resistance	$R$	2 k $\Omega$
Switching frequency	$f_s$	50 kHz
Line frequency	$f_l$	60 Hz
Sum voltage	$V_s$	450 V
Peak line voltage	$V_p$	170 V

steady-state error. In this work, the optimization of the PIDF of the current loop is carried out. The heuristic search algorithms Stochastic Hill Climbing (SHC) and Simulated Annealing (SA) are employed to determine the respective proportional, integral and derivative constants. In this way, the Power Factor (PF) provides the objective function for the optimization process.

The derivation of the state equations for the half-bridge boost rectifier can be found in [17, 18], in this way, without taking into account losses in the half-bridge boost rectifier and taking  $d$  as the duty cycle, a simplified model is given by the following equations:

$$\frac{di}{dt} = \left( \frac{2d-1}{2L} \right) v_s + \frac{1}{2L} v_d + \frac{1}{L} v_g \quad (1)$$

$$\frac{dv_s}{dt} = - \left( \frac{2d-1}{C} \right) i - \frac{2}{RC} v_s \quad (2)$$

$$\frac{dv_d}{dt} = - \frac{1}{C} i, \quad (3)$$

where  $v_s$  and  $v_d$  are the sum and difference of voltages  $v_1$  and  $v_2$ , respectively. Additionally, in Table 1, the parameters of the voltage-doubler boost rectifier used in the simulation are found, where the circuit parameter, the symbol, and the respective value are observed.

Finally, MATLAB is used for the simulation model where the simulation time is 20 min, which imposes a significant restriction to perform the controller optimization. In this way, heuristic algorithms based on an individual were chosen in a way that the optimization could be carried out during the simulation. Considering the above, the heuristics algorithms used are stochastic hill climbing and simulated annealing.

### 3. Stochastic hill climbing

Stochastic Hill Climbing (SHC) is considered a heuristic method employed in optimization to determine a suitable solution that may not be the global optimal; however, it can be an acceptable solution in reasonable time [19]. The SHC algorithm serves in maximization and minimization problems for a real function exploring different values of decision variables [20].

According to [19, 20], SHC is a heuristic algorithm that employs a population of one individual (state). Considering the search space, the initial solution is usually selected randomly. The exploration of solutions is made by producing a random change in the current

individual (solution). In this way, the new individual is contrasted with the previous state. Hence the new state replaces the previous one when an improvement in the objective function is observed. This process is repeated until reaching a certain value of the objective function or when a maximum number of evaluations are attained [21].

The generic steps for a stochastic hill climbing algorithm are:

- Step 1: Randomly determine the initial state (solution).
- Step 2: Apply successor function to the current state randomly.
- Step 3: Evaluate the current state.
- Step 4: Determine the difference between the old and the new state. If the new state is better, then accept this as the current solution.
- Step 5: If the termination conditions are reached, continue to Step 6; otherwise, repeat from Step 2 (until the current state stops changing or the number of iterations is reached).
- Step 6: Finalize and return the optimal solution.

### 4. Simulated annealing

Simulated Annealing (SA) is a heuristic employed in optimization to reach a suitable approximation to the optimal value of a real function. In cases when the problem is minimization, the global optimum will be the one for which the objective function has the smallest possible on the search space [22].

SA is a versatile optimization algorithm used in different fields; for example, in [23], it is combined with a particle swarm algorithm to improve global optimization capabilities. Another example is seen in [24] applied in a hybrid way with a genetic algorithm for multi-objective optimization problems. Finally, an application in neural networks can be seen in [25], where it is used for training and parameter setting.

According to [20, 22], the SA algorithm is rooted in the physical annealing process for steel and ceramics, a process that consists of heating a material (to annealing temperature) and later cooling the material to modify the physical features (desired structure). Heat increases the atom's energy allowing move from its initial state (local minimum) to a state with lower energy than the initial one (global minimum). Slow cooling allows a greater opportunity for recrystallizing in configurations with lower energy than the initial state [20].

Considering the physical phenomenon, Equation (4) allows to determine the probability associated with the energy increase. Using the Boltzmann constant  $k$ , it is possible to calculate  $P(\Delta E)$  for a given temperature  $T$  and energy magnitude  $\Delta E$ .

$$P(\Delta E) = e^{-\frac{\Delta E}{kT}} \quad (4)$$

The simulated annealing approach is appropriate for problems having several local minima such that algorithms like Gradient Descent (GD) always converge to the same local minimum. In this algorithm is considered an initial temperature  $T_0$ , which descends progressively having different alternatives like:

- Linear reduction:  $T = T - \alpha$ .
- Geometric reduction:  $T = T\alpha$ .
- Slow-decreased:  $T = \frac{T}{1+\alpha T}$ .

Each function reduces the temperature in a different way (rate) considering the setting parameter  $\alpha$ . Any solution that satisfies the requirements for an acceptable solution can be used as the subject of the evaluation.

Considering a neighbor for the current solution (state), a new solution is chosen randomly. The new solution is accepted if the performance difference between the old and new solutions is greater than zero (the new solution is superior). If the cost difference is smaller than zero (the old solution is superior), a random value in the interval  $[0, 1]$  is generated. If the random number falls below the threshold determined by the energy Equation (5), the new solution is approved.

The generic steps for a simulated annealing algorithm are:

- Step 1: Randomly determine the initial solution (state), and considering a criteria choose the initial temperature  $T = T_0$ .
- Step 2: Choose and set up the reduction function for temperature (linear, geometric or slow-decreased rule).
- Step 3: Decrease the temperature according to  $\alpha$ .
- Step 4: Apply successor function to the current state randomly.
- Step 5: Determine the variation between the existing and new state.
- Step 6: If the new state (solution) is better, then take this as the current state; otherwise, generate a random value in the interval  $[0, 1]$  and accept the new solution if the random value is under the threshold obtained from the energy Equation (5).
- Step 7: If the termination conditions are reached, continue to Step 8; otherwise, repeat from Step 3 (until the current state remains unchanged or the number of iterations is reached).
- Step 8: Finalize and return the optimal solution.

In the SA optimization algorithm, Equation (4) is adapted to Equation (5), where  $T$  is the temperature and  $\Delta J$  is the change in the objective function. In this way, probability  $P$  can be determined to accept the new state.

$$P = \begin{cases} 1 & \text{if } \Delta J \leq 0 \\ e^{-\Delta J/T} & \text{if } \Delta J > 0 \end{cases} \quad (5)$$

According to [20], and regarding Equation (5), when the temperature is higher, a worse solution can be accepted. This feature is associated with the exploration, namely allowing to evaluate different solutions, although they do not improve the objective function. When the temperature is lower, the probability of taking a worse state decreases, which is associated with exploitation, namely searching for better objective function values.

## 5. Optimization process

Traditional algorithms based on gradients are a suitable option given their mathematical support; nonetheless, they converge to local minima [15]. On the other hand, heuristic algorithms allow a better explanation of the search space of which there are based on several individuals (population) such as genetic algorithms and particle swarms; however, simulated annealing and stochastic hill climbing are only based on one individual [16].

Considering the time required for the simulation of a controller configuration, the optimization is carried out online, performing variations of the plant to obtain an improvement in the response of the plant. To carry out controller optimization, in the traditional approach, a separate simulation is made for each group of parameters. In this approach, during the same simulation, the performance of the system is evaluated for a group of parameters.

The SA and SHC algorithms are chosen to perform an online optimization since these only require evaluating the objective function (plant dynamics) once in each iteration. If algorithms are used with several individuals, it is necessary to evaluate the plant for each individual, which requires a setting of the plant to an initial state. In this way, it is not necessary to restart the plant to the initial configuration and the current state of the plant can be used to continue with the optimization process.

In this order, it is optimized the discrete PID controller parameters  $P$ ,  $I$ , and  $D$  given by Equation (6), where  $T_s = 20 \times 10^{-6}$  is the sample time and  $N = 59.56 \times 10^3$  the coefficient for the derivative filter.

The sampling time value ( $T_s = 20 \mu\text{s}$ ) is equal to switching period of the half-bridge boost rectifier, since the highest frequency in the input current of the rectifier is approximately 5 kHz. According to the criterion of Nyquist, the sampling frequency should be at least twice this frequency, hence a sampling frequency of 50 kHz is chosen. The filter coefficient  $N$  of the derivative filter is given by  $N = (T_s G)^{-1}$  considering the sampling period  $T_s$  (previously calculated) and the filter gain  $G = 0.84$  (close to unity).

$$C(z) = P + I \frac{T_s z + 1}{2 z - 1} + D \frac{N}{1 + NT_s \frac{z}{z-1}} \quad (6)$$



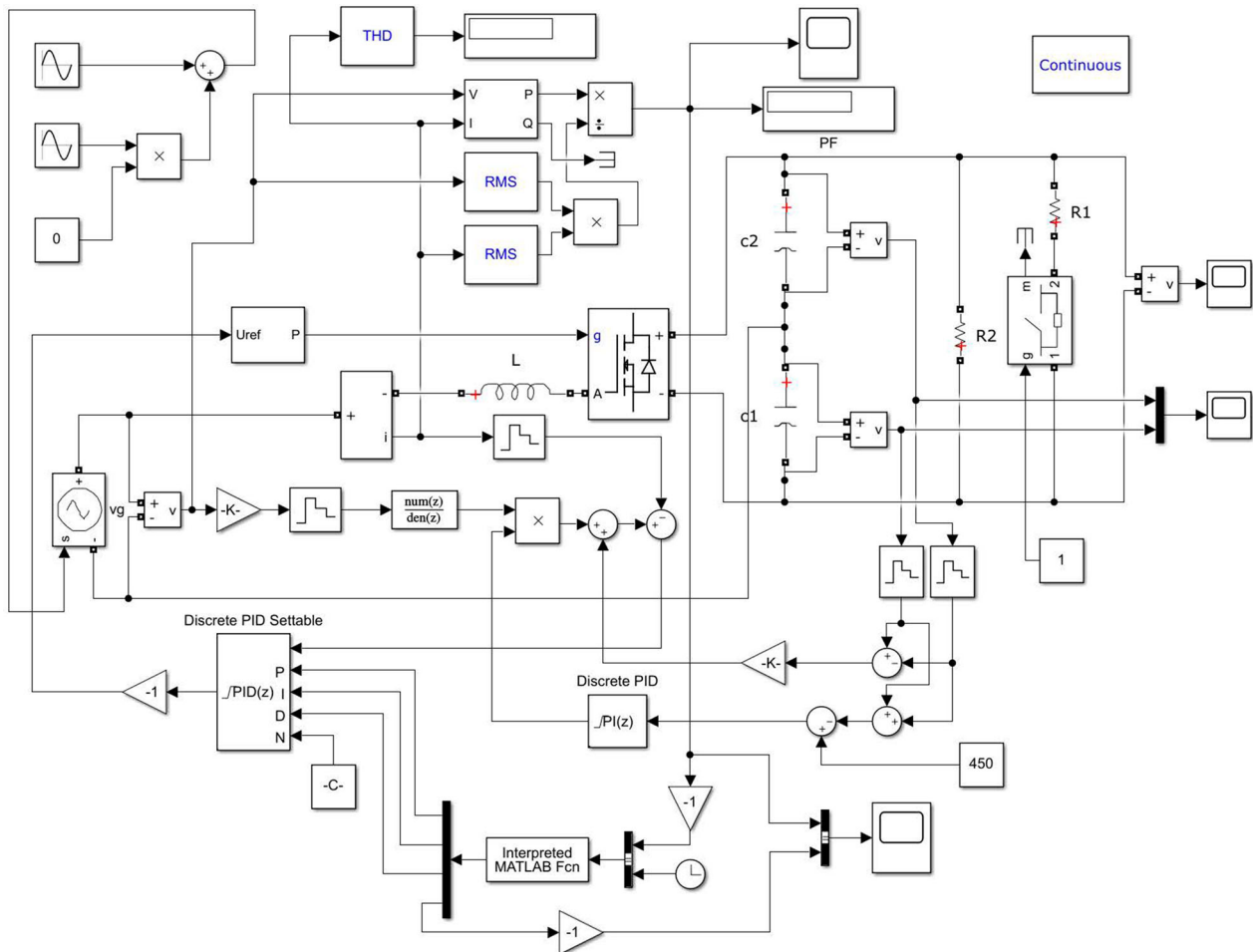


Figure 2. Simulation diagram.

The model implementation was made in MATLAB 2018b using *simulink* and the toolbox of *simscape* and *simscape electrical*. Figure 2 displays the simulation diagram observing the function employed during simulation to adjust the parameters of the PID controller. The implementation was done on a personal computer Toshiba Satellite C660-2FE, processor Intel Core i5, 2.4 GHz with 6GB of RAM, and running Windows 10.

As observed in Figure 2, the simulation time is entered in the optimization function block to establish the moments when the algorithm must change the parameters in the function that performs the parameter adjustment. It is also worth noting that the variables used in the optimization function must be of a global type so that their values can be read and written at any time during the system simulation.

For the optimization process during the system simulation, the function employed for optimization changes the parameters configuration of the PID controller in such a way that the value of the objective function is determined, then the optimization algorithm chooses another possible solution to evaluate.

Using SHC, if an improvement in the objective function is observed, the new configuration is maintained;

otherwise, the previous configuration is returned to later evaluate a new one. Meanwhile, using SA considering the probability value given by energy Equation (5), a solution that does not produce a better result is accepted. The steps for online optimization are as follows:

- Step 1: Initial parameters configuration.
- Step 2: Perform the simulation for the respective iteration  $k$ .
- Step 3: Obtain the response system and the objective function value.
- Step 4: Applied the respective optimization algorithm (SHC or SA).
- Step 5: Update the PID parameters according to the optimization algorithm.
- Step 6: If the finalization criterion is meet then finish; otherwise, return to Step 2.

The finalization criteria considered is the number of iterations ( $K = 20$ ). In addition, the objective function corresponds to the negative value of the power factor, namely  $J = -PF$ . In this way, the PF is calculated using Equation (7), where  $P$  is the active power,  $S$  is the apparent power, and  $\phi$  is the phase shift between voltage and

current.

$$PF = \frac{P}{S} \quad (7)$$

Considering the displayed in [8], the suitable initial values for the controller are  $K_p = 0$ ,  $K_i = 100$ , and  $K_d = 0$ ; however, tuning methods such as is presented in [26, 27] can be used to determine a suitable configuration of the PID controller that serves as the initial configuration. To set the simulated annealing algorithm is observed that the change in the objective function (using stochastic hill climbing) is between  $0.005 < \Delta J < 0.7$ . In this order  $T_0 = 3$  and  $\alpha = 0.15$  were used for a linear temperature decrease taking 20 iterations. Thus, it is important to select an appropriate value of  $\alpha$  for large changes to the objective function in the first iterations and small adjustments in the last iterations.

## 6. Results

Regarding the stochastic behavior of SCH and SA algorithms, conventionally, 20 runs are performed to obtain a usable result [28]. Table 2 displays the statistical values obtained for the time used in the optimization process, having the maximum, minimum, mean, and standard deviation (SD) values. As can be seen, it takes a total of 150.0277 h, that is, 6.2512 days, to complete the collection of the results of all the executions of the optimization algorithms.

For the implementation of the optimization process, the initial search point (controller parameters) is determined considering a nominal system operation according to the controller setting given in [17].

Table 3 shows the resulting statistical values for 30 runs of optimization algorithms. This table shows the maximum, minimum, mean, and standard deviation (SD). In this table, it can be seen that similar results are obtained using the two algorithms; however, the best result is obtained with SA.

In order to present the results in a qualitative way, the best configuration obtained is used to carry out the simulation of the converter, obtaining Figures 3

**Table 2.** Statistics of the results obtained for simulation time in hours.

Measure	SCH	SA
Max	3.6606	4.0993
Min	3.3030	3.7418
Mean	3.5277	3.9737
SD	0.1024	0.1065
Total	70.5532	79.4745

**Table 3.** Statistics of the results obtained for  $J$ .

Measure	SCH	SA
Max	-0.8528	-0.8780
Min	-0.9932	-0.9934
Mean	-0.9692	-0.9595
SD	0.0330	0.0250

and 4 for stochastic hill climbing, and Figures 5 and 6 for simulated annealing. These figures seek to show the algorithm search process and the system's behavior during this process.

Regarding the results obtained with stochastic hill climbing, Figure 3 presents the improvement in power factor throughout the optimization process of each execution of the optimization algorithm. For example, taking an execution of the optimization algorithm, Figure 4 displays the system behavior and optimization record for the power factor values.

Considering the results obtained employing simulated annealing, Figure 5 displays the improvement in power factor during the optimization process for each of the executions of the optimization algorithm. As an example taking an execution (run) of the optimization process, Figure 6 displays the system simulation and optimization record for the power factor obtained.

Taking the best configuration obtained using SA, the PID controller parameters are  $K_p = 0.0896$ ,  $K_i = 1.0702 \times 10^3$ , and  $K_d = 3.0682 \times 10^{-6}$ . Using these values is performed the system simulation obtaining the results in Figures 7 and 8. Noticeably, in this simulation, the dynamics of the controller consider the voltage and current converter, as well as the voltage regulation waveform.

Figure 7 displays the rectifier input voltage and current simulation ( $v_g, i_g$ ) using the parameters from Table 1 and the optimal values of the PID controller. In this figure, the voltage and current waveforms are noticeably close in phase. The power factor achieved is 0.9934, which is consistent with what is shown in Figure 7.

Meanwhile, Figure 8 displays the controller response observing the converter output voltage, as well as the voltage capacitors observed in the half-bridge. As can be seen, an adequate regulation of the output voltage is achieved, and also a suitable balance of the voltage of the capacitors.

Regarding comparisons with related works, reference [11] reported a power factor greater than 0.99, while reference [12] reported an achievement of 0.99. However, these topologies differ from the one proposed in this study. It should be noted that both references [11] and [12] correspond to recent works. On the other hand, in reference [13] a PFC converter identical to the one proposed was presented, achieving a power factor less than 0.99. The power factor of the proposed work is 0.9934, which is comparable with the results obtained in references [11, 12]. Meanwhile, when comparing the proposed work with reference [14], it can be stated that the power factor achieved is better compared to the obtained in [14]. It is also worth noting that the two topologies of the employed converters are different. The converter considered in this paper presents a zero at the origin (linear model [17]), while the converter in [14] presents a nonminimum-phase zero (linear model).

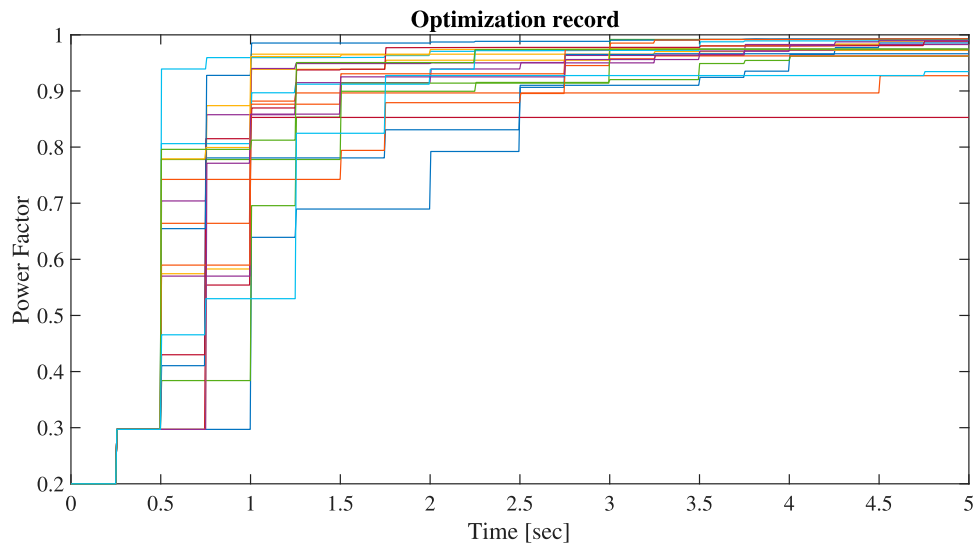


**Figure 3.** Improvement in power factor.

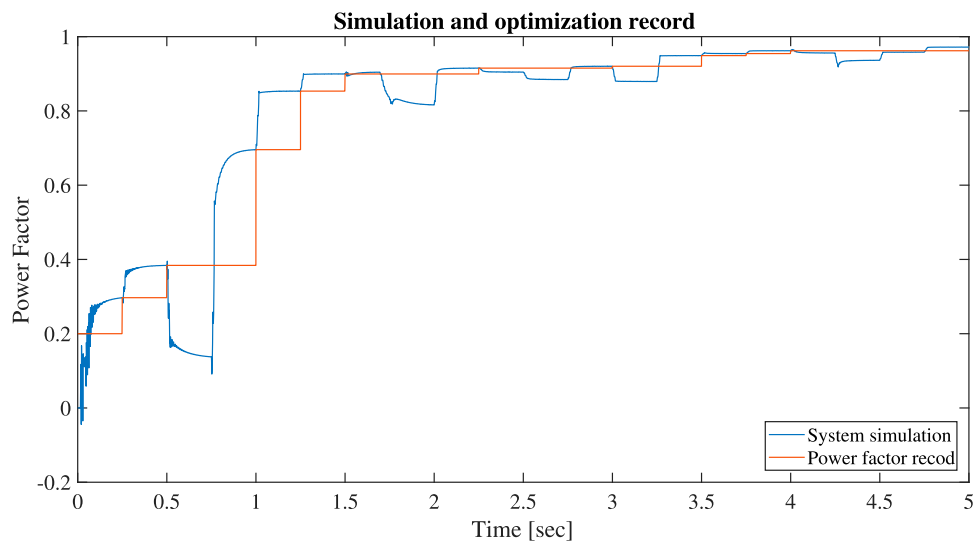


**Figure 4.** System simulation and optimization record.

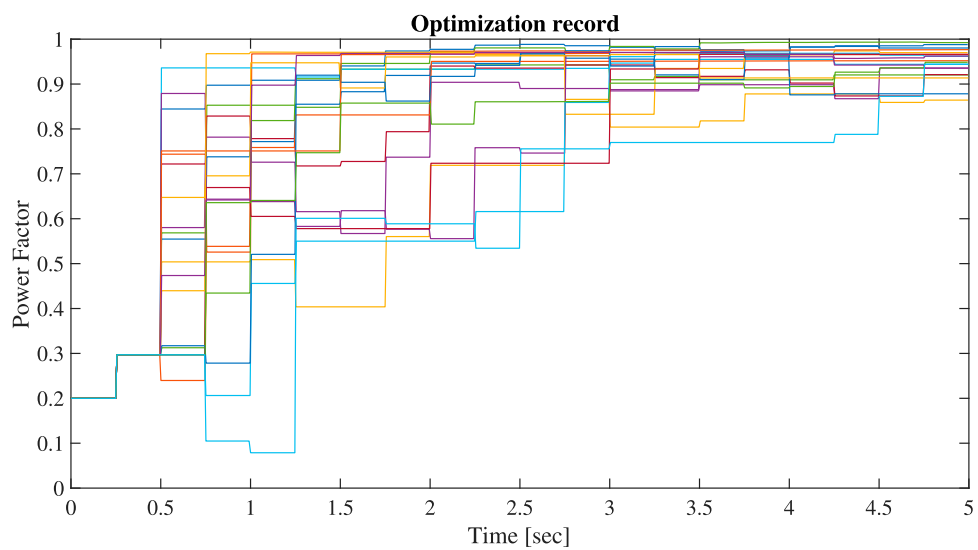


**Figure 5.** Improvement in power factor.



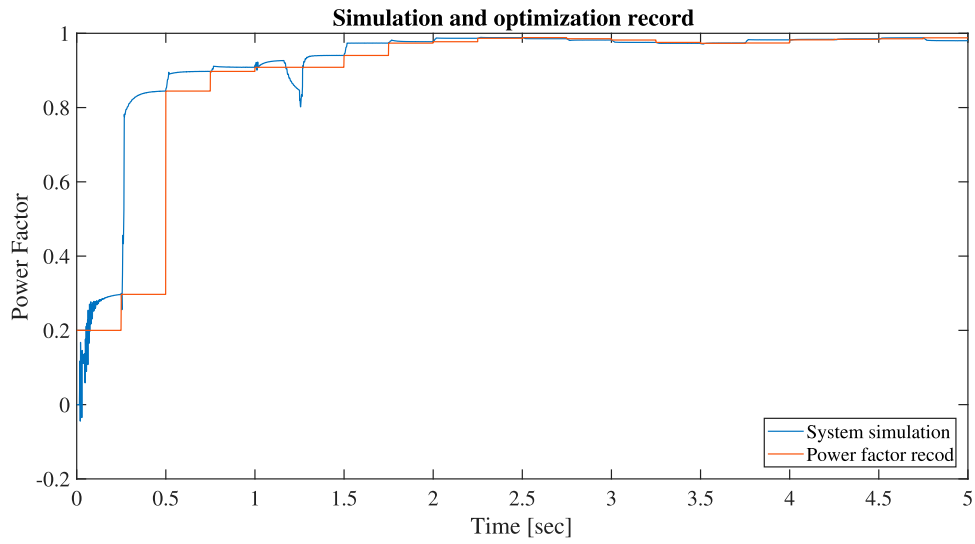


Figure 6. System simulation and optimization record.

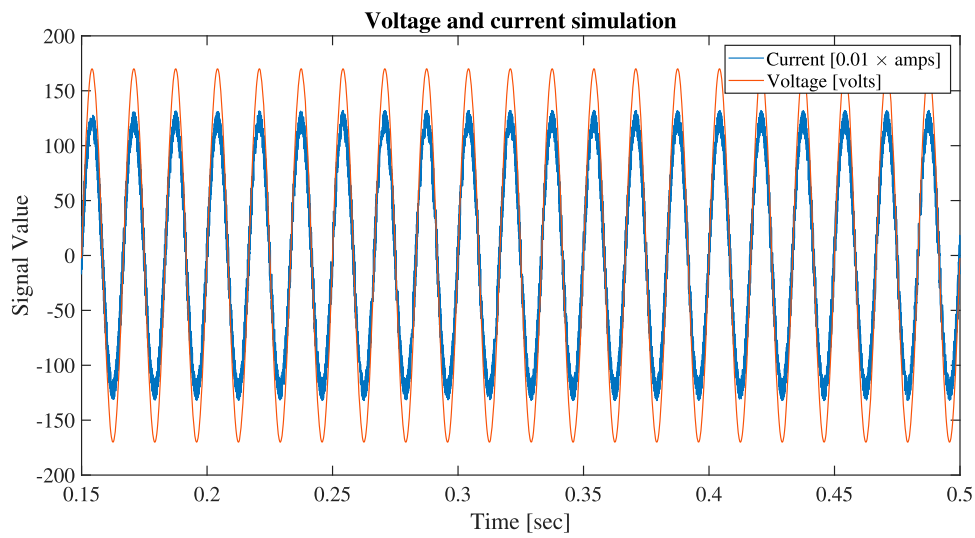


Figure 7. Input voltage and current simulation.

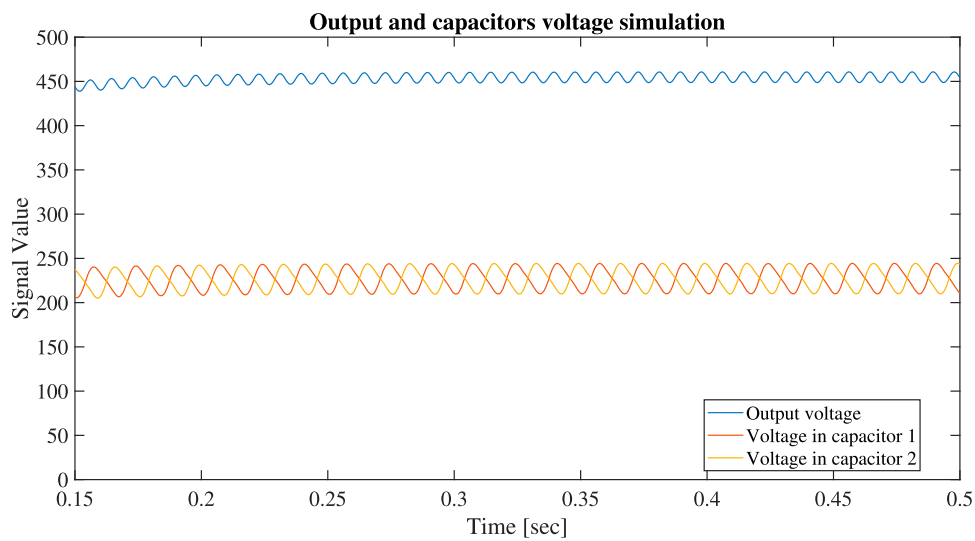
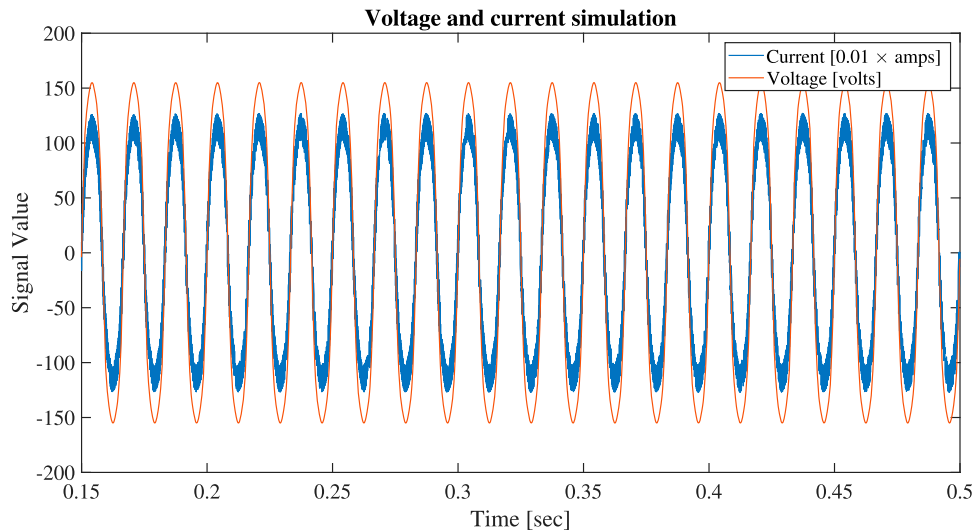


Figure 8. Output converter voltage response and capacitors voltage.



**Figure 9.** Input voltage and current simulation for a non-sinusoidal input voltage.

**Table 4.** Comparison of current harmonics regarding IEC 61000-3-2 standard.

Harmonic No.	IEC standard	Without distortion	With distortion
3	2.30 A	0.022270 A	0.086880 A
5	1.14 A	0.014640 A	0.033230 A
7	0.77 A	0.004869 A	0.003100 A
9	0.40 A	0.002048 A	0.003720 A

In addition, to observe the behavior of the converter for a non-sinusoidal input voltage (source with distortion), the generator connected to the input is  $v_g = 170 \sin(2\pi 60t) + 20 \sin(6\pi 60t) + 5 \sin(10\pi 60t)$ , obtaining a PF of 0.9827; the input voltage and current waveforms are presented in Figure 9. These results show that the power factor is high for both sinusoidal and non-sinusoidal voltage. Furthermore, the PID constants obtained with the optimization process allow reaching a power factor close to unity. Reviewing Figures 7 and 9, the input current waveform follows the input voltage waveform, indicating near zero steady state-error for both cases.

Finally, regarding the International Electrotechnical Commission (IEC) standards, Table 4 displays the comparison results considering the cases of voltage source with and without distortion. This table observed the current harmonics values obtained (in amperes) and the maximum value allowed according to IEC 61000-3-2 standard, where the device classification corresponds to class A (equipment not included in other classes) [29]. As observed in Table 4, the maximum values of the harmonics according to the standard are met. In addition, the iTHD without source distortion is 0.1141, and with source distortion is 0.1423, thus having a difference of 0.0282 when the distortion at the source is considered.

## 7. Discussion

Considering that the converter requires time for stabilization and there may be increases in the current flowing through the semiconductors when they are switched on, as well as voltage stress when they are switched off, this poses a limitation when implementing the hardware optimization process. Therefore, this study presents an approach to optimize the converter controller during the system operation itself through simulation. Another limitation in this work is the lack of real features of semiconductors, such as dead time, switching, and conduction losses.

Algorithms based on single individual were used due to the limitations in the operation of the converter. Although this work is conducted at the simulation level, it can serve as a basis for further hardware development. For the implementation of the algorithms, it is necessary to consider those values producing system instability. In this way, restrictions are included for the controller parameters.

Although the implementation developed is carried out at a simulation level, it can be implemented online in a real implementation, where the improvement of the system is obtained progressively during the operation of the plant (without restarting the plant). Also, it must be kept in mind that in a real implementation, the parameters may vary over time; thus, if this process is carried out continuously when the plant presents a variation in its parameters, the optimization process can change the controller configuration to find new values that allow improving the objective function. In this way, the proposed process acts as an adaptive scheme when plant variation occurs.

This approach can be used to perform an online adjustment of the controller in such a way that it can

correct the operation of the converter when plant variation occurs, improving the robustness of the system when having uncertainties in the plant. This aspect can be addressed in future work.

## 8. Conclusions

This work approaches the online optimization process of power systems when it is impossible to carry out a separate execution of each system configuration since the system requires time for its stabilization.

In this implementation, it was possible to optimize the parameters of the PID controller used in the converter. For this, it was necessary to propose an online optimization strategy during the operation (simulation) of the system.

An adequate dynamic behavior of the converter is observed with the optimized controller. The proposed scheme avoids evaluating configurations that could cause some damage to the system since it performs a progressive adjustment considering the current configuration.

In a later work, simulations that involve dead time, switching, and conduction losses can be carried out, as well as real hardware implementation of this optimization scheme in a way that compares real and simulation results. Also, the possibility of using a supervised system to control the power flow could be addressed, including a hardware implementation.

## Acknowledgments

The authors express gratitude to the Universidad Distrital Francisco José de Caldas, and to the Universidad ECCI.

## Disclosure statement

No potential conflict of interest was reported by the author(s).

## ORCID

Jhon Bayona  <http://orcid.org/0000-0001-6688-1988>

Nancy Gélvez  <http://orcid.org/0000-0003-3334-6959>

Helbert Espitia  <http://orcid.org/0000-0002-0742-6069>

## References

- [1] Espitia H, Machón-González I, López-García H. Optimization of a Takagi-Sugeno fuzzy controller for voltage regulation of a DC-AC single-phase inverter. In: 2019 IEEE Workshop on Power Electronics and Power Quality Applications (PEPQA), Manizales, Colombia; 2019. p. 1–6.
- [2] Rashid MAZA, Ponniran A, Noor MKR, et al. Optimization of PFC cuk converter parameters design for minimization of THD and voltage ripple. *Int J Power Electron Drive Syst (IJPEDS)*. 2019;10(1):514–521. doi: [10.11591/ijpeds.v10.i1](https://doi.org/10.11591/ijpeds.v10.i1)
- [3] Hiendro A, Yusuf I, Junaidi J, et al. Optimization of SHEPWM cascaded multilevel inverter switching patterns. *Int J Power Electron Drive Syst (IJPEDS)*. 2020;11(3):1570–1578. doi: [10.11591/ijpeds.v11.i3](https://doi.org/10.11591/ijpeds.v11.i3)
- [4] Patil MD, Vadirajacharya K, Khubalkar S. Design of fractional order controllers using constrained optimization and reference tracking method. *Int J Power Electron Drive Syst (IJPEDS)*. 2020;11(1):291–301. doi: [10.11591/ijpeds.v11.i1](https://doi.org/10.11591/ijpeds.v11.i1)
- [5] Abidin Z, Muttaqin A, Maulana E, et al. Buck converter optimization using P&O algorithm for PV system based battery charger. *Int J Power Electron Drive Syst (IJPEDS)*. 2020;11(2):844–850. doi: [10.11591/ijpeds.v11.i2](https://doi.org/10.11591/ijpeds.v11.i2)
- [6] Tayyab Yaqoob M, Khairil Rahmat M, Marwangi Mohamad Maharum S, et al. A review on harmonics elimination in real time for cascaded h-bridge multilevel inverter using particle swarm optimization. *Int J Power Electron Drive Syst (IJPEDS)*. 2021;21(1):228–240.
- [7] Abdelkader Mekki A, Kansab A, Matallah M, et al. Super-twisting sliding mode controllers based on D-PSO optimization for temperature control of an induction cooking system. *Int J Power Electron Drive Syst (IJPEDS)*. 2020;11(2):1055–1064. doi: [10.11591/ijpeds.v11.i2](https://doi.org/10.11591/ijpeds.v11.i2)
- [8] Bayona J, Gélvez N, Espitia H. Design, analysis, and implementation of an equalizer circuit for the elimination of voltage imbalance in a half-bridge boost converter with power factor correction. *Electronics*. 2020;9(12):1–23. doi: [10.3390/electronics9122171](https://doi.org/10.3390/electronics9122171)
- [9] Kushwaha R, Singh B. A bridgeless isolated half bridge converter based EV charger with power factor pre-regulation. In: 2019 IEEE Transportation Electrification Conference (ITEC-India), Bengaluru, India; 2019. p. 1–6.
- [10] Malschitzky A, Agostini E, Bitencourt Nascimento C. Integrated bridgeless-boost nonresonant half-bridge converter employing hybrid modulation strategy for led driver applications. *IEEE Trans Ind Electron*. 2021;68(9):8049–8060. doi: [10.1109/TIE.2020.3013749](https://doi.org/10.1109/TIE.2020.3013749)
- [11] Du Y, Bhat AKS. Analysis and design of a high-frequency isolated dual-tank LCL resonant AC-DC converter. In: 2014 International Power Electronics Conference (IPEC-Hiroshima 2014 – ECCE ASIA), Hiroshima, Japan; 2014. p. 1721–1727.
- [12] Li H, Yuan Z, Yang Z, et al. A control scheme for a combo 1-Ph/3-Ph PFC rectifier with improved leg utilizations. *IEEE Trans Power Electron*. 2023;38(12):15131–15136. doi: [10.1109/TPEL.2023.3317178](https://doi.org/10.1109/TPEL.2023.3317178)
- [13] Ghosh R, Narayanan G. A simple analog controller for single-phase half-bridge rectifier. *IEEE Trans Power Electron*. 2007;22(1):186–198. doi: [10.1109/TPEL.2006.886621](https://doi.org/10.1109/TPEL.2006.886621)
- [14] Guarnizo JG, Torres-Pinzón CA, Bayona J, et al. MPSO-based PID control design for power factor correction in an AC-DC boost converter. *Automatika*. 2023;64(4):893–902. doi: [10.1080/00051144.2023.2225918](https://doi.org/10.1080/00051144.2023.2225918)
- [15] Mataifa H, Krishnamurthy S, Kriger C. Volt/var optimization: a survey of classical and heuristic optimization methods. *IEEE Access*. 2022;10:13379–13399. doi: [10.1109/ACCESS.2022.3146366](https://doi.org/10.1109/ACCESS.2022.3146366)
- [16] Desale S, Rasool A, Andhale S, et al. Heuristic and meta-heuristic algorithms and their relevance to the real world: a survey. *Int J Comput Eng Res Trends*. 2015;351(5):2349–7084.
- [17] Bolívar F, Díaz N, Bayona J. Design and implementation of a digital pid controller with pre-compensation loop for a half-bridge PFC boost converter. *UIS Ingenierías*. 2020;19(1):179–192.

- [18] Bayona JF, Chamorro HR, Sanchez AC, et al. Linear control of a power factor correction rectifier in half-bridge configuration. In: IEEE CACIDI 2016 – IEEE Conference on Computer Sciences, Buenos Aires, Argentina; 2016. p. 1–6.
- [19] Sivanandam SN, Deepa SN. Introduction to genetic algorithms. New York: Springer Berlin Heidelberg; 2007.
- [20] Kulkarni P, Joshi P. Artificial intelligence: building intelligent systems. Delhi: PHI Learning; 2015.
- [21] Rosete-Suárez A, Ochoa-Rodríguez A, Sebag M. Automatic graph drawing and stochastic hill climbing. In: Proceedings of the 1st Annual Conference on Genetic and Evolutionary Computation – Volume 2, GECCO'99. San Francisco(CA): Morgan Kaufmann Publishers Inc; 1999. p. 1699–1706.
- [22] Millán Páramo C, Begambre Carrillo O, Millán Romero E. Propuesta y validación de un algoritmo simulated annealing modificado para la solución de problemas de optimización. *Rev Int Métodos Numér Cálculo Diseño Ing.* 2014;30(4):264–270.
- [23] Yang S, Wang H, Xu Y, et al. A coupled simulated annealing and particle swarm optimization reliability-based design optimization strategy under hybrid uncertainties. *Mathematics.* 2023;11(23):1–24.
- [24] Sun X, Guo S, Guo J, et al. A pareto-based hybrid genetic simulated annealing algorithm for multi-objective hybrid production line balancing problem considering disassembly and assembly. *Int J Prod Res.* 2024;62(13):4809–4830. doi: [10.1080/00207543.2023.2280696](https://doi.org/10.1080/00207543.2023.2280696)
- [25] Engin Kuruoglu E, Lin Kuo C, Kin Victor Chan W. Sparse neural network optimization by simulated annealing. *Frankl Open.* 2023;4:100037. doi: [10.1016/j.fraope.2023.100037](https://doi.org/10.1016/j.fraope.2023.100037)
- [26] Panda RC. Synthesis of PID tuning rule using the desired closed-loop response. *Ind Eng Chem Res.* 2008;47(22):8684–8692. doi: [10.1021/ie800258c](https://doi.org/10.1021/ie800258c)
- [27] Panda RC. Introduction to PID controllers: theory, tuning and application to frontier areas. Rijeka: IntechOpen; 2012.
- [28] Babor M, Senge J, Rosell CM, et al. Optimization of no-wait flowshop scheduling problem in bakery production with modified PSO, NEH and SA. *Processes.* 2021;9(11):1–20. doi: [10.3390/pr9112044](https://doi.org/10.3390/pr9112044)
- [29] IEC 61000-3-2:2018. Electromagnetic Compatibility (EMC). Limits for Harmonic Current Emissions (equipment Input Current  $\leq 16$  A Per Phase). Number Part 3-2 in International standard. International Electrotechnical Commission, 2018.